Raytracing meets Maxwell's Equations: integrating micro- and macro-optical design

Steven A. Miller, Breault Research Organization (BRO), Tucson, AZ, USA
James Pond, Lumerical Solutions, Vancouver, BC, Canada
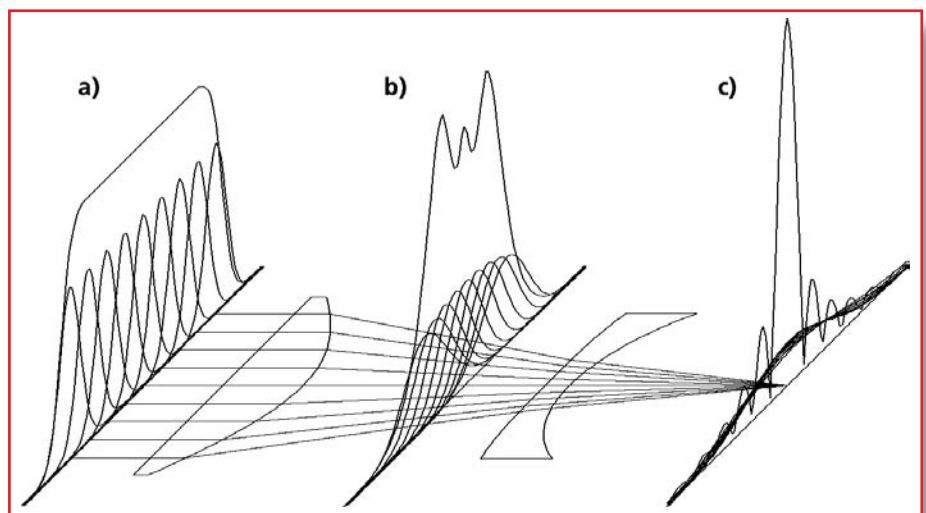**Bernhard Michel, Simuloptics GmbH, Schwabach, Germany**

Advances in technology have always presented product developers with unique challenges. This is particularly true in the optics industry, for example in the task of integrating micro-scale optical components into marketable products. While designers have at their disposal a wide range of sophisticated software tools, no single software package can operate in both the macroscopic realm of system design and in the microscopic realm of wavelength-scale devices. This article will introduce both approaches – microscopic and macroscopic – for the reader to understand their mutual strengths and limitations. Critical aspects of the interoperability of these complementary tools will be discussed along with several application examples.

In response to a growing customer demand, Breault and Lumerical are integrating their optical softwares to grant optical engineers access to a broad range of design and analysis tools for tasks previously considered inaccessible in applications such as micro-optics, optical audio & video devices, projection systems, bio-optics instrumentation and more.

1 Software for macro- and micro-scale optics

Conventional ("sequential") raytracers serve for designing optics by means of geometrical tracing of optical rays. BRO's Advanced Systems Analysis Program (ASAP) is a non-sequential raytracer which means that the order in which a ray hits physical objects is not predefined but is instead calculated during beam propagation. Additionally, coherent propagation of gaussian beams is implemented in ASAP, providing comprehensive abilities to simulate optical effects including scattering, diffraction, reflection, refraction, absorption, and polarization within the context of macroscopic three-dimensional optical and mechanical systems.

The design, optimization and verification of micro- and nano-scale photonic components and integrated optics, such as planar waveguides and devices, as well as photonic crystal fibers, optical storage, microlenses, etc., requires software based upon different methods, such as
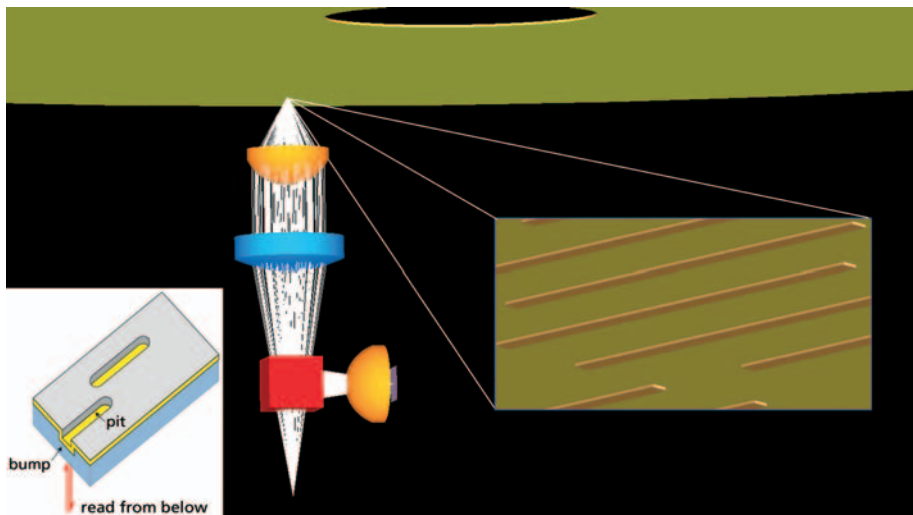

Figure 1: Principle of Gaussian beam decomposition. The incident field (a) is decomposed into many gaussian beamlets which are raytraced through the optical system. By coherent superposition of the beamlets, the field can be reconstructed at any plane (b, c)

Lumerical's finite different time domain solver FDTD Solutions and the fully-vectorial mode solver MODE Solutions. FDTD algorithms solve the time-dependent Maxwell's equations. They require field quantities to be calculated in grid steps equivalent to small fractions of a wavelength. As a result, spatial dimensions of an FDTD simulation are restricted by practical limitations on computational resources. On the other hand, raytracing methods are inapplicable in (sub-) wavelength-scale

regimes as a result of the approximations they employ. A simulation environment which adequately deals with both macroscopic and microscopic optical components therefore requires a marriage of the two approaches, raytracing and FDTD.

2 Gaussian beam decomposition

ASAP addresses physical optics by means of gaussian beam decomposition [1], as sketched in **Figure 1**. An incident field is

Figure 2: *Coherent output from a laser diode passes through a cube beamsplitter and two focusing elements onto the disk surface (top). The reflected/diffracted light passes back through the focusing elements, is diverted by the cube beamsplitter to a focusing optic and finally onto a detector*

decomposed into a set of gaussian beamlets. The individual gaussian beamlets are then sent through the optical system by geometric raytracing, accurately accounting of path length. The optical field can be reconstructed at any plane in the system by coherent superposition of the gaussian beamlets. The field itself can be almost arbitrary, but the individual Gaussian beamlets it is composed of must obey the paraxial approximation. Consequently, their divergence angles θ relative to their propagation directions must be small, and due to the beam divergence relationship

$$\theta = \lambda/(\pi w_o) \qquad \text{(Eq. 1)}$$

their waist diameters $2w_o$ must be larger than approximately 5-8 wavelengths λ [2]. Therefore, wavelength–scale features cannot be adequately sampled this way.

There are generally two reasons for calculating the complex field in ASAP. Primarily, the field is calculated as a final result; thus, it is possible for instance to obtain the field's intensity distribution, phase distribution, or polarization state at any planar interface, image plane or component of interest.

Secondly, there is often the need to adjust the spatial sampling of the field. This can be done by decomposing the field into a new (finer or coarser) set of gaussian beamlets. Such a field decomposition has to be used in order to obtain the sub-wavelength spatial resolution needed for the data exchange with FDTD Solutions. While decomposition of fields in ASAP can be positional or directional, depending upon dimensions involved, only directional

decomposition is applicable for the data exchange with FDTD Solutions.

3 Interoperability with FDTD Solutions

Interaction of electromagnetic waves with wavelength-scale structures is the forte of Finite Difference Time Domain simulation codes. FDTD algorithms are useful for design and analysis in a wide variety of applications involving the propagation of electromagnetic radiation within complicated and dispersive media. It is especially useful for describing radiation incident upon or propagating through structures with strong scattering or diffractive properties.

Interoperability between ASAP's raytracing code and FDTD Solutions is achieved by exchanging the electric field distribution from one to the other program on a rectangular interface window, a so called "sample plane" or "measurement plane". Typically, ASAP calculates the field to be "injected" into a micro-optics system. FDTD Solutions uses this field to compute the interaction within the micro-optics system. The resulting field is then either the final result of the calculation or it is passed back to ASAP to further propagate it through a macroscopic optical system.

Another aspect of interoperability is that the FDTD algorithm is inherently time-dependent, while ASAP calculates a time-independent electric field, only. Since FDTD Solutions solves Maxwell's equations, the magnetic component of the field must be reconstructed when importing data. The

time-independent fields are transformed into wavelets with finite frequency bandwidth, and their extension in time and space is simulated. Fourier transformation of the time-dependent fields and stripping their magnetic field component renders the time-independent field distribution, which can be exported back to ASAP. Specific commands simplify the exchange of complex field data between the programs.
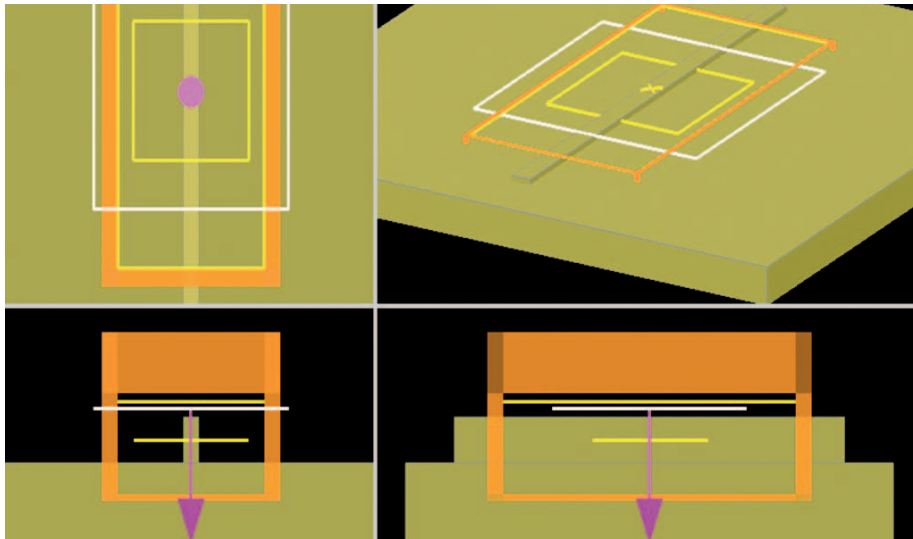
4 Application examples

In the following, we will provide an overview of three representative applications illustrating interoperability of software using microscopic and macroscopic approaches. First, the digital versatile disk (DVD) player serves as an example of a two-way exchange between ASAP and FDTD Solutions. Examples involving a CMOS lenslet array and a photonic crystal fiber illustrate the ability to introduce wavefronts from real optical systems into these devices rather than the idealized sources to which these simulations are normally confined.

4.1 DVD Reader

A typical DVD optical read head as modeled in ASAP is shown in **Figure 2**. Interaction with the DVD surface is necessarily an intermediate step in this simulation. Note that microscopic DVD surface features (see left-hand inset in Figure 2) need not be included in the ASAP model. Their geometry is constructed entirely within FDTD Solutions. For this demonstration, the area of interest consists of a basal plane ("landing") and a single depression ("pit"), or – when seen from the read-side – an elevation ("bump") of width 320 nm, a height of 120 nm, and length of 8 µm as shown in the right-hand inset in Figure 2. The optical properties of the entire structure are defined by a wavelength-dependent model for gold immersed in PMMA.

The simulation begins in ASAP by tracing the source rayset to a "measurement plane" defined in close proximity to the DVD surface. The complex electric field vector is calculated at that window and exported to FDTD Solutions. In this case, an area 4 µm · 4 µm located 140 nm before the landing insures that all the focused energy is captured at a position 20 nm (one FDTD grid spacing) before the bump. Choosing a larger window for the field calculation would gain only little additional information, but would increase runtime considerably. On the other hand, any clipping caused by under-sizing the window could lead to diffraction effects at other locations within the optical system for which there is no physical basis. Having

Figure 3: Simulation geometry generated in FDTD Solutions. The ASAP source (grey box with purple arrow) is imported into this geometry, and the measurement plane (yellow rectangle) records the reflected signal. The simulation volume (orange cubic volume) encloses all these elements

exported the complex electric field to FDTD Solutions, the ASAP simulation is temporarily suspended.

The simulation then proceeds independently in FDTD Solutions by importing the ASAP source into a geometry that has been designed in FDTD Solutions, as shown in **Figure 3**. Running the FDTD simulation results in the field at the measurement plane for the reflected signal being stored and converted into an ASAP-readable format. The simulation resumes in ASAP by first importing the FDTD field and decomposing it into Gaussian beamlets. After tracing these beamlets to the detector plane, the beam profile can be observed with a final field calculation.
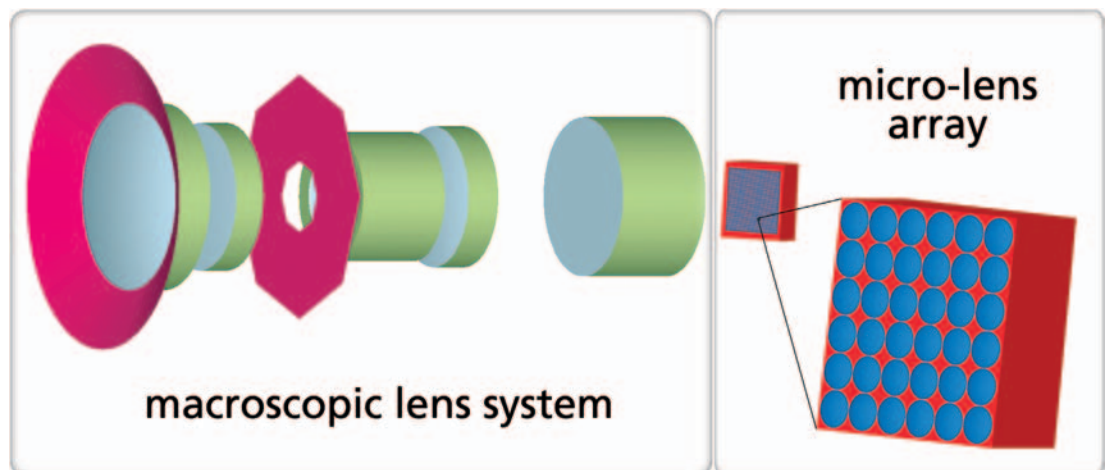
For the specific parameters used in this example, the return beam remained central, showing a 14 dB amplitude reduction in the presence of the bump as compared to the landing only.

4.2 CMOS detector with micro-lens array

The next application example involves a digital camera system using a CMOS detector fitted with a micro-lens array (**Figure 4**). The f/2.8 camera lens [3,4] of focal length 5.26 mm has a corner-to-corner FOV of 49.2°. The CMOS detector array features a pixel spacing of 4 µm. The micro-lenses have a radius of curvature of 4 µm and are positioned above each detector pixel.

This simulation is typical of a one-way field transfer from ASAP to FDTD Solutions. For this type of problem, the ASAP model doesn't need to contain details of the microstructure. Specifically, in this case the micro-lens array and CMOS detector are virtually "absent" for ASAP. It traces rays incident on the camera aperture from selected field points to a measurement plane located just in front of the micro-lens array. As in the DVD simulation, the complex field incident on one micro-lens and its nearest neighbors is calculated in a window 5-10 λ across and exported to FDTD Solutions, where the remainder of the simulation takes place.

As an illustration of possible questions that can be examined with FDTD Solutions, consider a brief study of crosstalk amongst adjacent CMOS pixels. **Figure 5** represents graphical output from FDTD Solutions showing irradiance in adjacent pixels. The pixels are positioned 16 µm behind the micro-lens array surface, and the response is assumed to be proportional to the integrated irradiance over the full pixel surface. Dead space between pixels was ignored. For each field point, the plots compare horizontal and diagonal half-pixel misalignment of the Airy disk to the array lenslets.

While micro-lens arrays can help increase the fill factor of digital cameras, leading to large pixel counts and increased signal to noise ratio (SNR), they can also contribute to pixel cross-talk which widens the sensor point spread function (PSF) and increases the overall blur of the image [5]. The combined analysis of the macroscopic lens system and the microlens array allows the designer to optimize the camera by trading off the requirements for a high SNR and a narrow system PSF - two requirements that are often difficult to achieve simultaneously.

4.3 Coupling efficiency of a photonic crystal fiber

Our final application example relates to a commercially available photonic crystal fiber used for applications in non-linear optics. The software MODE Solutions is engaged to find its guided modes. Design-

Figure 4: Geometrical arrangement of camera system with lens array (and CMOS detector at rear of array package). The insert shows a magnified 6x6 sub-array

ers might use this outcome to specify parameters of an optimum beam delivery system or assess the degradation in coupling efficiency arising from a less-than-ideal lens, which can be modeled in ASAP. The result of a brief study confirmed the assumption that smaller spot sizes allow for a maximum coupling efficiency to the fiber, while a larger spot size can be advantageous in reducing the alignment sensitivity of the coupling efficiency.
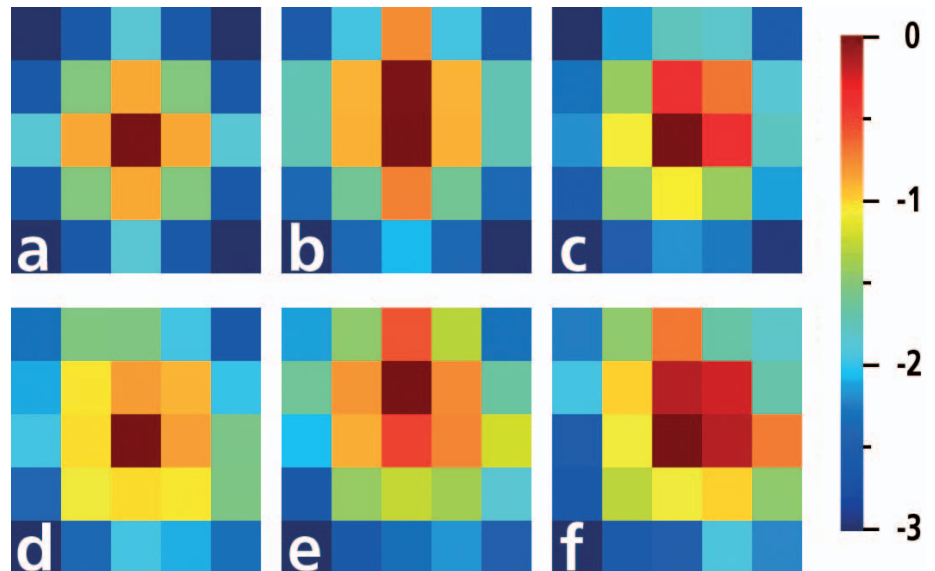
A particularly useful feature of MODE Solutions is its capability to import scanning electron microscope (SEM) images. **Figure 6** shows the cross section of an NL-15-670 photonic crystal fiber manufactured by Crystal Fibre A/S (*www.crystal-fibre.com*). Its index profile was used in the aforementioned alignment sensitivity study.

5 Conclusion

The purpose of this article was to demonstrate the synergy effects arising from the combination of the non-sequential raytracer ASAP with the finite difference time domain software FDTD Solutions. Through the interoperation of both softwares, optical systems can now be modeled that contain both macro- and microscopic components – which offers fascinating new opportunities for optical system design.

Figure 5: Logarithm of the irradiance signal in adjacent CMOS detector pixels, 16 µm behind the microlens array, for on-axis illumination (a-c) and 20° off-axis illumination (d-f). Figures a (central pixel) and d (pixel closer to the edge of the chip) show the ideal case when the spot is at the center of the pixel. Figures b, c, e, and f show the case when the spot is mis-aligned by 0.02176° in different directions

Literature References:

[1] A. Greynolds, *Vector Formulation of Ray-Equivalent Method for General Gaussian Beam Propagation*, Proceedings of SPIE: Current Developments in Optical Engineering and Diffractive Phenomena 679 (1986): 129-133

[2] F. Pedrotti, L. Pedrotti, W. Bausch, H. Schmidt, *Optik: Eine Einführung*, Prentice Hall, München 1996; Chapter 22

[3] U.S. Patent 5,706,141, issued Januar 1998

[4] J. Brian Caldwell, Patent Design: *High Resolution CCD Lens*, Optics and Photonics News, p. 45, March 1998

[5] T.Q. Pham, L.J. van Vliet, K. Schutte, *Influence of signal-to-noise ratio and point spread function on limits of super-resolution*, in: E.R. Dougherty, J.T. Astola, K.O. Egiazarian (eds.), *Image Processing: Algorithms and Systems IV*, Proc. IS&T, SPIE's 17th Annual Symposium Electronic Imaging, San José, CA, USA, 16.-20. Jan. 2005, Proc. SPIE, vol. 5672, 169-180
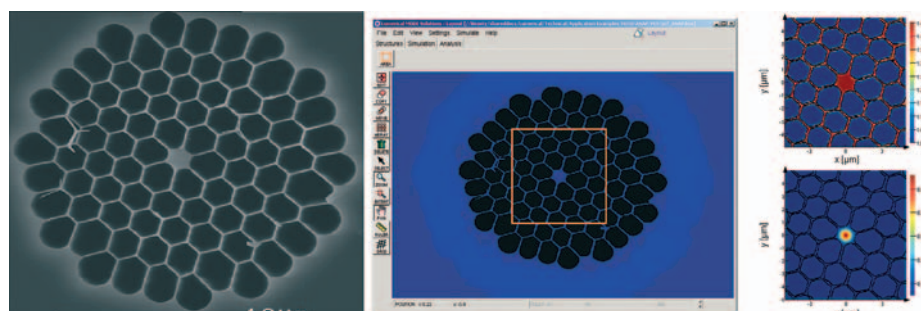
Author contact:

Dr. Steven A. Miller
Software Technical Support
Breault Research
Organization (BRO)
6400 East Grant Road,
Suite 350
Tucson, AZ 85715, USA
Tel. +1/520/721-0500
Fax +1/520/721-9630
eMail: support@breault.com
Internet: www.breault.com

Dr. James Pond, CTO
Lumerical Solutions
Suite 660 –
789 West Pender Street
Vancouver BC, Canada,
V6C 1H2
Tel. +1/604/733-9006
Fax +1/604/733-3188
eMail: jpond@lumerical.com
Internet: www.lumerical.com

Dr. Bernhard Michel
Simuloptics GmbH
German representative of
BRO and Lumerical
O`Brien Str. 2
91126 Schwabach
Germany
Tel. +49/9122/830300
Fax +49/9122/830303
eMail: info@simuloptics.de
Internet: www.simuloptics.de
www.lightscattering.de

Figure 6: Importing SEM images allows the designer, among other things, to take representative manufacturing defects into account when calculating mode distribution and coupling efficiency. Left: Cross-sectional SEM image of the photonic crystal fiber NL-15-670 (courtesy of Crystal Fibre A/S); center: Cross-section after importing into MODE Solutions; Right top: Refractive index mesh of the photonic crystal fibre; Right bottom: Mode profile of the fundamental mode